Engineering and Technology Journal
Journal homepage: https://etj.uotechnology.edu.iq

Optimal operational conditions of PLA/PBAT mixed matrix membrane for the treatment of oily wastewater

Maryam Y. Ghadhban[a], Khalid T. Rashid[a], Adnan A. Abdulrazak[a], Hicham Meskher[b*], Yacine Benguerba[c], Emad A. Yousif Al-Sarraj[d], Qusay F. Alsalhy[a]

[a] Chemical Engineering Dept., University of Technology-Iraq, Alsina'a street, 10066 Baghdad, Iraq.
[b] Division of Process Engineering, College of Science and Technology, Chadli Bendjedid University, 36000, Algeria.
[c] Laboratoire de Biopharmacie Et Pharmacotechnie (LPBT), Ferhat Abbas Sétif 1 University, Sétif, Algeria.
[d] Chemical Engineering Dept., Engineering College, University of Al-Nahrain-Iraq, Baghdad, Iraq.
*Corresponding author Email: h.meskher@univ-eltarf.dz

HIGHLIGHTS

- A novel method uses Hesperidin (HSP) with PLA/PBAT MMMs to remove oil by simulating oily wastewater.
- RSM and ANOVA were applied to enhance the technique's large-scale effectiveness.
- The impact of HSP NPs content, oil concentration, and pressure on MMMs performance was optimized.
- PLA/PBAT/HSP-based MMMs had optimal efficiency with 121 LMH flux and 98.53% oil rejection.
- Optimal conditions for HSP MMMs were 0.03 wt.% HSP, 158.28 ppm oil concentration, and 3.5 bar pressure.

ARTICLE INFO

Handling editor: Raed A. Al-Juboori

Keywords:
PLA/PBAT membrane; Response surface methodology; Oil/water separation; Hesperidin; Design-Expert® software

ABSTRACT

This study aims to optimize the operational variables influencing the incorporation of Hesperidin nanoparticles (HSP NPs) into poly(lactic acid)/poly(butylene adipate-co-terephthalate) (PLA/PBAT) for manufacturing mixed matrix membranes (MMMs) for oily wastewater treatment. An optimization method was employed to determine the optimal values for key process factors to achieve specific flux and rejection rates exceeding required levels. Statistical techniques such as response surface methodology (RSM) and analysis of variance (ANOVA) were used to enhance performance on a larger scale. This research investigated the impact of operating parameters on the flux and oil rejection of PLA/PBAT/HSP membranes across all samples. The variables studied included HSP NPs content (0-0.05 wt.%), oil concentration (100-300 ppm), and transmembrane pressure (1.5-3.5 bar). A mathematical model for calculating flux and rejection (%) was developed. The findings indicated that the PLA/PBAT/HSP-based MMMs demonstrated optimal efficiency, achieving a flux of 121 LMH and oil rejection of 98.53%. The optimal conditions for the HSP MMMs were 0.03 wt.% HSP, an oil concentration of 158.28 ppm, and a pressure of 3.5 bar yielded the best response. The results show that the PLA/PBAT/HSP membranes exhibited enhanced flux and separation properties, making them suitable for treating oily wastewater in various applications.

1. Introduction

The availability of clean water is an essential requirement for humanity, and as the global population continues to expand, the demand for freshwater is steadily rising [1,2]. However, the supply of freshwater resources is diminishing steadily, raising concerns that these resources may not meet the daily demand for fresh water in the near future. Therefore, the global focus on the accessibility of clean water has significantly increased [3-5].

The problem of oily wastewater has long been recognized as a significant concern in water pollution. Industries release substantial quantities of oily wastewater discharges into rivers [6,7]. Upon reaching the water, these substances have a detrimental effect on ecosystems and organisms. The sources of this pollution encompass several industries, such as oil and gas, textile, food, metals, and petrochemical manufacturing [8-10].

http://doi.org/10.30684/etj.2024.150993.1774
Received 17 June 2024; Received in revised form 13 August 2024; Accepted 20 August 2024; Available online 03 September 2024
2412-0758/University of Technology-Iraq, Baghdad, Iraq

The uncontrolled release of oily wastewater has numerous negative effects on the surrounding environment, such as the contamination of surface and groundwater, the pollution of marine and soil ecosystems, and the release of hydrocarbon compounds and oil evaporation into the atmosphere, leading to air pollution [11,12]. In addition to its toxicity, oily wastewater can inhibit the growth of animals and plants and increase the possibility of cancer in humans [13,14]. Various methods have been developed to separate oily wastewater, such as flotation, coagulation, biological treatment, adsorption, and membrane separation [15-17].

Membrane filtration is regarded as a highly promising method for separating oil-water emulsions. The membranes display several advantages compared to other technologies, including but not limited to their superior ability to separate fine oil-water emulsions, the lack of need for more chemicals, great separation ability, cost economy, small size, and equipment flexibility [18,19]. Although membranes provide some benefits, they are affected by fouling and show little stability throughout the separation operation [20,21]. Modifying and functionalizing membrane surface enhances its characteristics and improves its performance, like selectivity and flux, hence improving its use [22-24]. One of the major developments in improving the hydrophilic nature of polymers biodegradability was achieved by incorporating nanomaterials into the polymeric matrix [25-27], such as metal oxides (Al_2O_3, TiO_2, SiO_2, ZnO, MgO, Fe_2O_3, and zeolite) [28,29].

A variety of green nanoparticles have been produced using eco-friendly and cost-effective techniques to use them in wastewater treatment applications like Acacia gum [30], Ginger extract [31], fibers of bamboo [32], gum Arabic [33], and a very wide range of natural materials [34-36]. From various green additives, hesperidin (HSP NPs) has been investigated for its possible utility to enhance membrane properties such as stability, flux, and rejection.

Considerable endeavors have been undertaken to improve the efficiency of MMMs to achieve optimal permeate flux, high rejection, and processing long-term viability. These demands identify the most favorable operating parameters for this process. Several parameters were selected for appropriate working conditions, including pressure, pH, feed concentration of solutes, incorporating additive quantity, and others. Meenakshi et al. [37] studied the impact of various operational factors on removing selenium from drinking water, including pH, feed concentration, cross-flow rate, and transmembrane pressure. The studied module achieved a high level of selenium separation (more than 98%) by using optimum operating parameters based on response surface methodology. Additionally, it maintained a consistently high flux of 140 LMH at an operating pressure of 14 bar.

Response surface methodology (RSM) optimizes processes when multiple elements and interactions influence the intended outcomes. Response surface methodology (RSM) is a valuable statistical and mathematical technique employed to enhance and optimize the experimental procedure influenced by multiple elements [38]. Therefore, RSM not only determines the most favorable value for each variable but also evaluates the relationships between them and their influence on one or more measurable outcomes [39-41].

The present study examines the optimization of operational parameters in the ultrafiltration process utilizing Hesperidin mixed matrix membrane. The investigation applied response surface methodology (RSM) and variance analysis (ANOVA). Herein, the study focused on optimizing different operating parameters such as HSP-NPs content (0-0.05 wt.%), oil concentration (100-300 ppm), and transmembrane pressure (1.5-3.5 bar), using Design-Expert® software. These experiments aimed to determine their impact on the membrane flux and oil rejection %. In addition, the study investigated how operating factors interact to optimize PLA/PBAT/HSP-based membrane performance.

2. Experimental

2.1 Reagents

Hesperidin (HSP) (MW 610.56) was purchased from Santa Cruz Biotechnology, USA. Dichloromethane (DCM) is obtained via Merck KGaA, a German company. PLA MW 80,000) and PBAT (MW 120,000) had been ordered from New Material Inc., Hubei BlueSky—Sodium Decyl Sulfate (SDS) obtained by India, HIMEDIA. Diesel oil is supplied from Al-Daura Refinery, Iraq/ Baghdad.

The solvent-nonsolvent (coagulation water bath) exchange rate during the phase inversion method. This leads to new pores forming.

2.2 PLA/PBAT/HSP-based membrane manufacturing

The mixed matrix membranes (PLA/PBAT/HSP) were synthesized using a process of non-induced phase separation, the rate at which solvents and nonsolvents (coagulation water baths) exchange in the phase inversion process. As noted in our previous work, this leads to new pores forming [42]. Table 1 shows the entire membrane composition. The PLA and PBAT polymers were dried at 50°C to eliminate residual moisture—next, 14 wt.% PLA and 4 wt.% PBAT were mixed in DCM solvent and stirred in a covered flask for a day [43]. Hesperidin concentrations ranging from 0 to 0.05 wt.% were employed during the preparation. Bath sonication was used to disperse the desired content of HSP in the cast solution, resulting in a homogeneous cast mixture. The gases were removed from the cast solution at a vacuum and cast utilizing a machine knife with a clearance spacing of 150 µm. After 4 min of evaporation, the glass surface was submerged in a water bath at 23±2 °C for 30 min. to complete the phase separation process. When removing the membrane, it was thoroughly rinsed in DI water to remove any residual solvent. These membranes were immersed in containers containing DI water and kept at ambient temperature till they were characterized, as shown in Figure 1.

Table 1: The composition of the membrane

Membrane code	PLA%	PBAT%	HSP%	DCM%
MR1	14	4	0	82
MR2	14	4	0.0125	81.9875
MR3	14	4	0.025	81.975
MR4	14	4	0.05	81.95

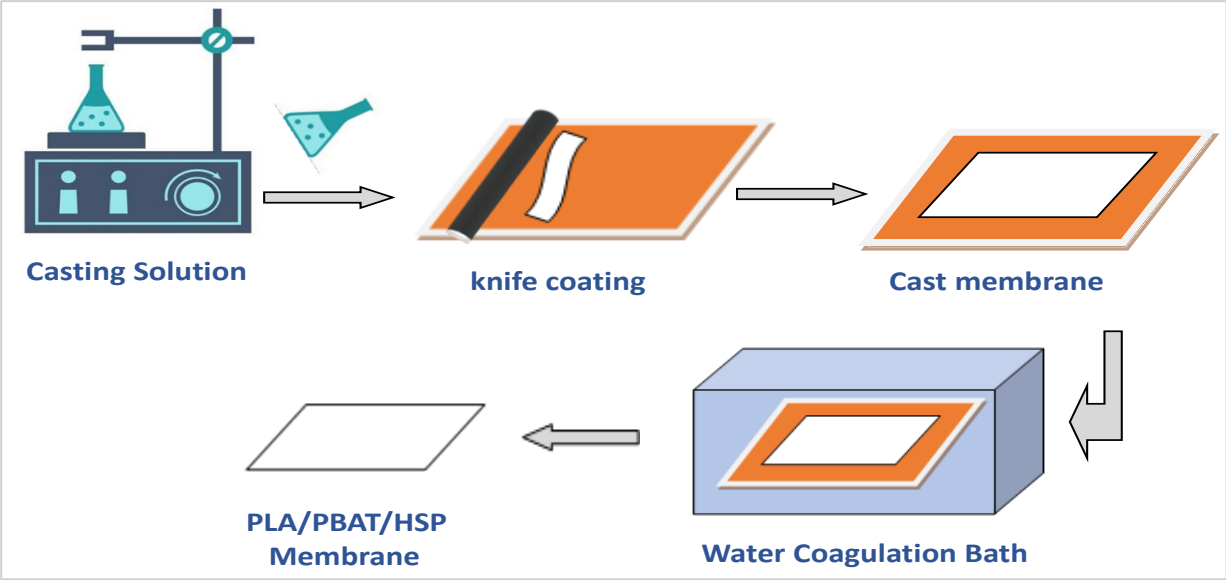

Figure 1: A schematic diagram of membrane preparation

2.3 Mixed matrix performance

The performance of the manufactured MMMs was assessed using a cross-flow filtering system with a membrane cell fitted with an active area of 24 cm^2. Firstly, DI water was utilized for compressing all membranes for 30 minutes at 2 bars, and then, the pressure decreased, and the flux was recorded at specified intervals using Equation 1 follows [44,45]:

$$J = \frac{Q}{At} \quad (1)$$

where J refers to the flux ($L/m^2.h$), Q is the total volume (L), t is the time (h), and A is the effective surface area (m^2).

Three different diesel oil concentrations (100, 200, and 300 ppm) were utilized to determine the efficiency of the prepared MMMs. When a feed solution was supplied through each membrane, the flux was recorded, and Equation 2 was employed for calculating the retention values as shown below [46,47]:

$$R\% = \left(1 - \frac{Cp}{Cf}\right) \text{x } 100\% \quad (2)$$

Cp and Cf are the oil concentrations in the permeate and feed solutions.

2.4 Experimental design

Response surface methodology (RSM) is a statistical and mathematical technique to develop a test series. The objective is to enhance the response, influenced by several independent factors [48,49]. Another advantage of the RSM design is the decreased trial requirement compared to a complete experimental design at an equivalent level. Furthermore, RSM's ultimate goal is to find the optimal conditions for the system's operation or to identify the region that meets the operating parameters. Regarding the "one factor at a time" approach, RSM helps reduce material costs and time [50-52].

The analyses were conducted using Design-Expert® software. The present study focused on optimizing different operational parameters, such as the concentration of HSP-NPs (0 to 0.05%), the transmembrane pressure (1.5 to 3.5 bar), and the oil feed concentration (100 to 300 ppm), to assess their impact on the flux and rejection percentage of the membranes.

Moreover, the study examined the combined influence of operational factors on the outcome. ANOVA is a statistical method that allows researchers to assess the effectiveness of developed models by providing statistical findings and diagnostic tests [38]. Table 2 shows the experimental information and variable symbols. A series of experiments were conducted utilizing the ultra-filtration membrane method, with each test modifying a single element to find the required operational parameters while keeping the remaining variables the same.

The optimization technique known as Response Surface Methodology aimed to investigate the impact of different parameters (predictors) on the flux and rejection percentage process. The specific information on the historical data of the 20 runs is provided in Table 3. These data points are utilized as design points to model and optimize the flux and rejection of oil.

Table 2: Code and levels of factors

Variables	Coded	Unite	Low level	High level
Oil concentration	A	Ppm	100	300
Pressure	B	Bar	1.5	3.5
Additive conc.	C	wt.%	0	0.05

Table 3: Experimental data points and response

Run	Conc. (ppm) (A)	Press. (bar) (B)	Addi. Conc. (wt.%) (C)	R (%)	F (LMH)
n	200	1.5	0.025	99	87
2	200	2.5	0.025	98.9	95.2
3	300	3.5	0.05	95.9	32
4	200	2.5	0.025	98.9	95.2
5	100	1.5	0.05	94.9	44.1
6	200	2.5	0.05	95.4	36
7	300	1.5	0	88.7	11.2
8	200	2.5	0.025	98.9	95
9	200	2.5	0	88.2	24.3
10	200	3.5	0.025	98.8	115
11	300	1.5	0.05	96.2	25
12	200	2.5	0.025	98.9	95.2
13	100	3.5	0	85	75.7
14	100	1.5	0	88	28.6
15	100	3.5	0.05	94.5	73.2
16	200	2.5	0.025	98.9	95.2
17	100	2.5	0.025	98	121
18	200	2.5	0.025	98.9	95.2
19	300	3.5	0	88.5	21.4
20	300	2.5	0.025	99	82

3. Results and discussion

3.1 MMMs filtration cross-flow evaluation

Each mixed matrix membrane (MMM) exhibited a higher pure water flux (PWF) than the pure membrane. The addition of green additives substantially impacted the flux characteristics, even with a small amount of HSP NPs. The findings indicated that the flux of water improved from 62 (LMH) for the initial membrane (MR1) to 102.7 (LMH) when 0.0125% of HSP-NPs were introduced. With the use of HSP-NPs, the PWF exhibited a significant increase, and the highest recorded value of 220.5 LMH was achieved for MR3.

As mentioned earlier, the rise in PWF was in line with the hydrophilicity measurements, porosity, and pore size of the prepared MMMs. The pure water flux was dropped by around 75.5 (LMH) after adding 0.05% (HSP-NPs). The high concentration of HSP-NPs has resulted in the blockage of the pore, leading to a decrease in PWF [53].

3.2 Regression models equation and ANOVA Analysis

The ANOVA analyses were performed using Design-Expert®. The analysis of variance (ANOVA) results for the flux and rejection (%), based on the HSP NPs wt.%, oil concentrations, and transmembrane pressure values, are presented in Table 3. Each predictor variable in the design layout has a corresponding specific p-value in the table of ANOVA results

These results were analyzed to predict a mathematical equation. The regression model equations for flux and rejection (%) are written as Equations 3 and 4 for mixed matrix membranes regarding the actual variables.

$$F = +95.66 - 17.10\,A + 12.14\,B + 4.91\,C - 7.37\,AB + 1.43\,AC - 2.65\,BC + 5.09\,A2 + 4.59\,B^2 - 66.26\,C^2 \quad (3)$$

$$R\,(\%) = +98.89 + 0.79\,A - 0.41\,B + 3.85\,C + 0.36\,AB - 0.1\,AC + 0.31\,BC - 0.38\,A^2 + 0.023\,B^2 - 7.08\,C^2 \quad (4)$$

Where F is the flux (LMH), R% is the rejection %, A is the oil concentration (ppm), B is the transmembrane pressure (bar), and C is the HSP NPs wt.%.

In Equation 3, positive factor terms indicate their positive impact, while negative factor terms indicate their negative impact on the flux. In Equation 4, a positive sign in the factor term indicates a positive impact, whereas a negative sign indicates a negative impact on the rejection.

The flux and rejection% models had a correlation coefficient R^2 value of 99.76% and 99.64%, respectively. Furthermore, the (adjusted) R^2 values were 99.54% and 99.32%, respectively. It is suitably elevated and in strong concurrence with the values of R^2. These data demonstrate that the flux and rejection% models are valid for statistics and can accurately predict UF MMMs performance. The regression analysis of the permeate flux and rejection% models demonstrates that the model's accuracy fits the information provided with good precision [54].

Furthermore, the predicted correlation coefficient R^2 (pred.) values closely align with the (adj.) correlation coefficient R^2 with each model, as indicated in Table 4. Consequently, both mathematical models incorporated important terms.

Table 4: ANOVA analysis of the flux and rejection

Membrane		Flux				Rejection			
Source	**DF**	**SS**	**MS**	**F-Value**	**P-value**	**SS**	**MS**	**F-Value**	**P-value**
Model	9	23624.01	23624.01	454.41	< 0.0001 Significant	424.42	47.16	310.31	< 0.0001 Significant
Oil Conc	1	2924.10	2924.10	506.20	< 0.0001	6.24	6.24	41.07	< 0.0001
Press	1	1473.80	1473.80	255.14	< 0.0001	1.68	1.68	11.06	0.0077
Add Conc	1	241.08	241.08	41.73	< 0.0001	148.22	148.22	975.35	< 0.0001
conc*press	1	435.13	435.13	75.33	< 0.0001	1.05	1.05	6.92	0.0252
conc*add	1	16.24	16.24	2.81	0.1245	0.28	0.28	1.85	0.2036
press* add	1	56.18	56.18	9.73	0.0109	0.78	0.78	5.14	0.0468
conc*conc	1	71.27	71.27	12.34	0.0056	0.39	0.39	2.58	0.1396
press* press	1	57.96	57.96	10.03	0.0100	1.420E-003	1.420E-003	9.347E-003	0.9249
add* add	1	12073.23	12073.23	2090.05	< 0.0001	137.74	137.74	906.37	< 0.0001
Residual	10	57.77	57.77			1.52	0.15		
Lack of Fit	5	57.73	57.73			1.52	0.30		
Pure Error	5	0.033	0.033			0.000	0.000		
Cor Total	19	23681.78				425.94			
Model Summary		Std. Dev.	R^2	Adj. R^2	Pred. R^2	Std. Dev.	R^2	Adj. R^2	Pred. R^2
		2.40	0.9976	0.9954	0.9638	0.39	0.9964	0.9932	0.9389

3.3 Effect of Pareto chart

The influence of the independent parameters and how they interact are illustrated in Pareto charts in Figure 2. The diagram illustrates the effect of many parameters on the oil/water flux and the rejection %. These factors include the concentration of oil (ppm) (referred to as factor A), the transmembrane pressure (referred to as factor B), and the concentration of additives wt.% (referred to as factor C) and, several interaction factors. Figure 2a demonstrates that the square term of the additive concentration (C^2) has a major impact on flux, followed by the effects of terms (A and B). The terms AB, C, A^2, B^2, BC, and AC have a lower effect on flux. Figure 2b illustrates that the additive concentration terms (C and C^2) have the greatest impact, whereas the terms (A, B, AB, A^2, BC, and AC) have a smaller effect on rejection (%). The (B^2) term does not have any potential influence.

The percentage contributions (PC%) were determined by utilizing Equation 5 [55]:

$$PC\% = \left(\frac{SS}{\Sigma SS}\right) \text{x } 100\% \quad (5)$$

where SS represents the sum of the squares for these variables, as seen in Table 5.

Based on the data shown in Table 6, it can be observed that the sequence of the factors' percentage contributions to the flux and rejection is consistent with the findings depicted in the Pareto chart.

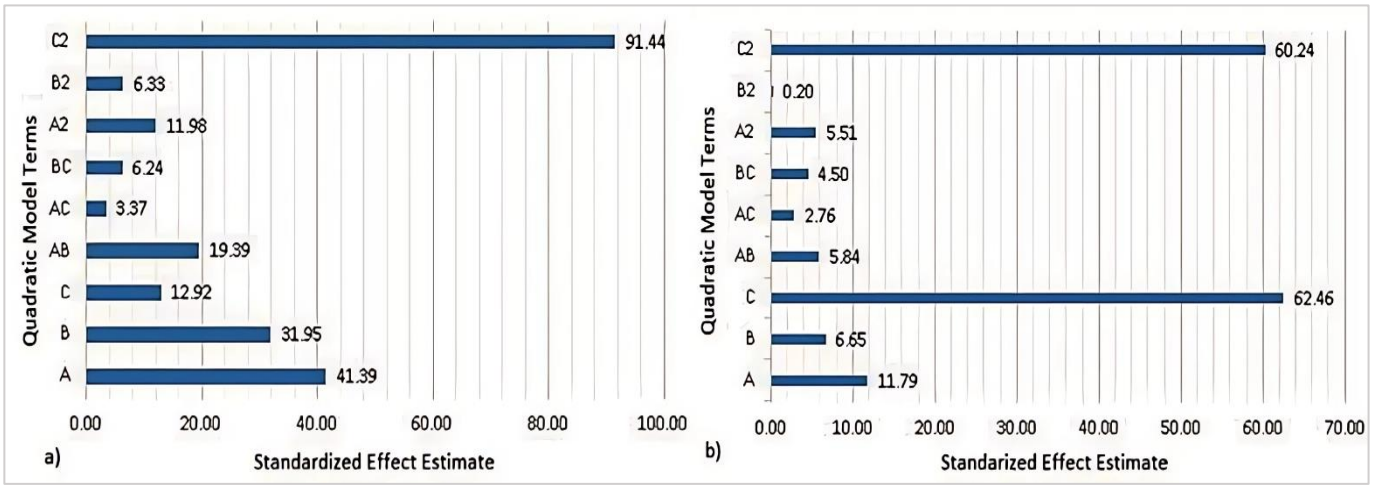

Figure 2: Pareto chart for (a) flux and (b) rejection (%)

Table 5: The (PC%) of variables for flux and rejection (%)

Source	A	B	C	AB	AC	BC	A^2	B^2	C^2
Flux	16.85	8.49	1.38	2.50	0.09	0.32	0.41	0.33	69.59
Rejection	2.10	0.56	50.01	0.35	0.09	0.26	0.13	0.0004	46.47

3.4 Main effects plot

Figures 3, 4, and 5 show how Design-Expert® software analyzed the impact of the experimental parameters and their interactions. One variable was changed to investigate the factor's impact, while the others remained unchanged. When varying the factor from the low to the high level, a zero slope indicates that the variable has a grace effect. Still, a slope of one indicates that the variable positively impacts the response.

Figure 3 depicts the connection between flux and rejection (%) for MMMs with a constant transmembrane pressure (3.5 bar) and the concentration of additive (0.03 wt.%). The flux was reduced with a rise in oil concentration (100 - 300 ppm). The accumulation of oil molecules over the membrane decreased flux Figure 3a [56,57]. Whereas the rejection (%) for MMMs grew when the oil content rose using (100 - 300 ppm). The presence of oil molecules over the membrane surface can create a thin, compact layer, raising the total rejection rate Figure 3b [58,59].

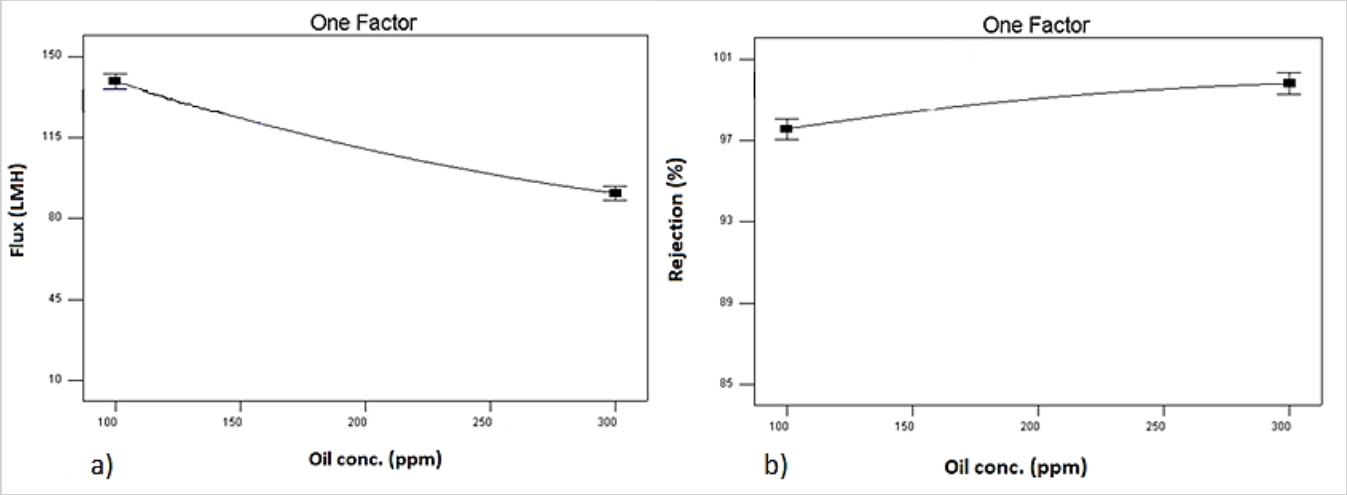

Figure 3: The oil concentration effect on (a) flux and (b) rejection% for MMMs at constant pressure is 3.5 bar, and the additive concentration is 0.03 wt.%

Figure 4 depicts how changing the pressure from 1.5 to 3.5 bar affects the flux and rejection % of MMMs at a constant oil concentration of 158.28 ppm and additive concentration of 0.03 wt.%. Flux increased as the pressure increased from 1.5 to 3.5 bar. With the diffusion and solution model, flux directly connects with the pressure differential through the membrane Figure 4a [60,61]. However, as shown in Figure 4b, the rejection % for the membrane decreased slightly as the pressure rose from 1.5 to 3.5 bar.

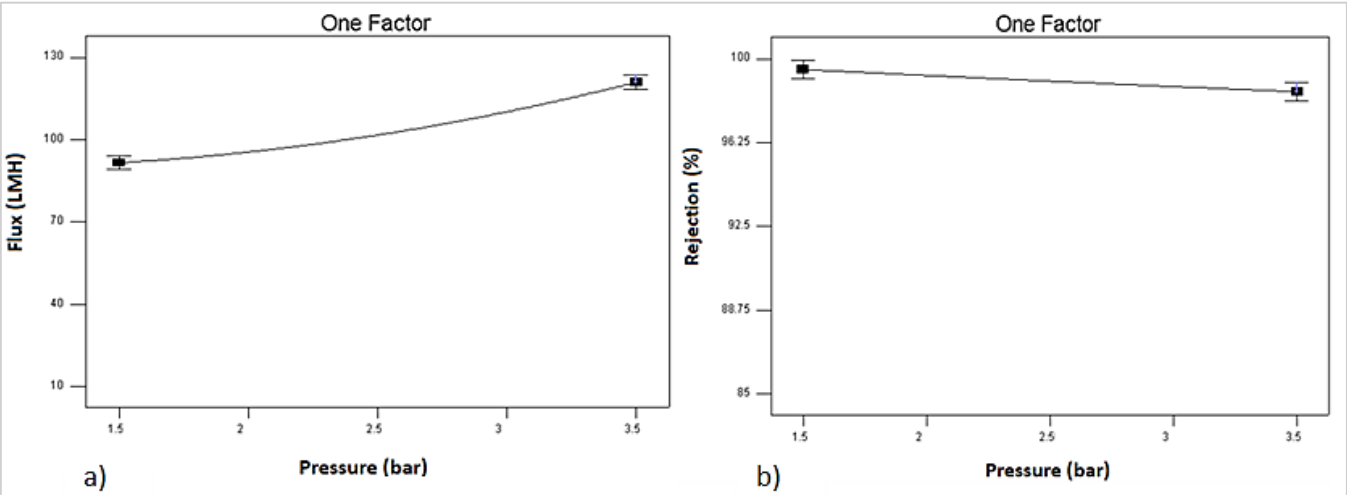

Figure 4: Transmembrane pressure affects (a) flux and (b) rejection% for MMMs at constant oil concentration 158.28 ppm and additives concentration 0.03 wt.%

Figure 5 demonstrates the effect of additive concentration on membrane flux and rejection % at a constant oil content at 158.28 ppm and 3.5 bar pressure. Figure 5a shows that the flux increased when the additive concentration rose by 0.03 wt.%. Increasing the concentration of HSP-NPs in the PLA/PBAT cast solution enhanced the membrane's porosity, average pore size, and hydrophilicity. On the other hand, raising the number of additives to 0.05 wt.% reduced the flux due to the HSP-NPs agglomeration on the surface of PLA/PBAT membranes, resulting in lower porosity, pore size, and hydrophilicity; that agglomeration was thought as the source of the flux decrease [62,63]. When obtaining the rejection % for MMMs, it was observed a rise in rejection as the additive concertation increased. This tendency might have been linked to hydrophilic HSP-NPs that improve membrane surface hydrophilicity [64].

Furthermore, as the concentration of HSP-NPs was elevated to 0.05 weight percent, the rejection of (oil-water) emulsion reduced Figure 5b. The decrease in oil rejection could be related to rising HSP-NP aggregation levels. It causes some faults to be created during the membrane fabrication process, which might have an adverse effect on the rejection of the membrane [65].

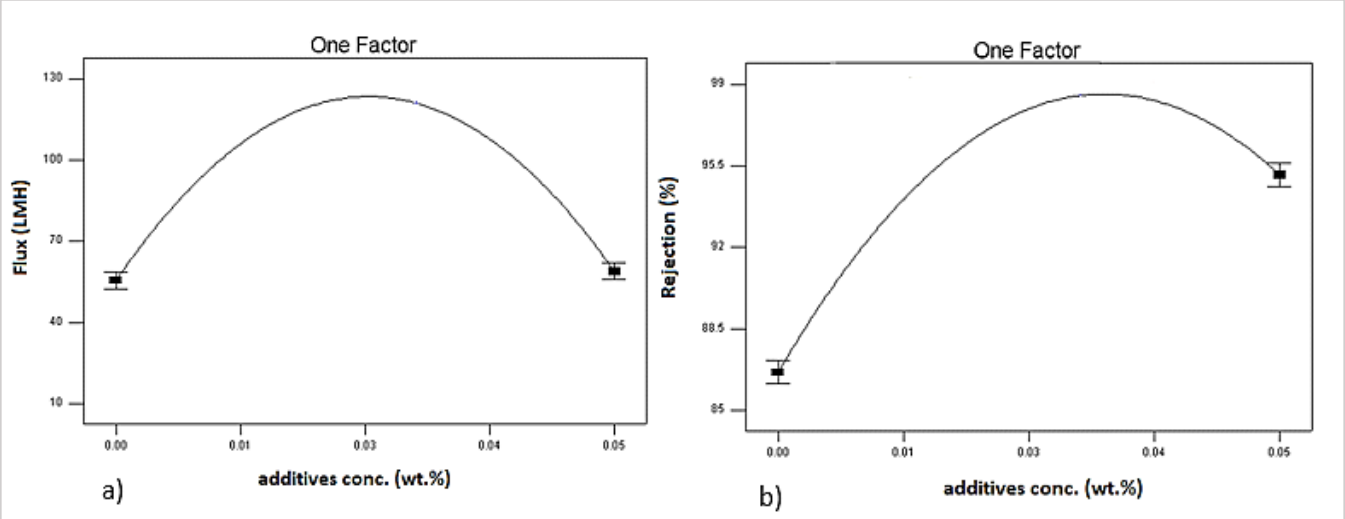

Figure 5: Additives concentration effect on (a) flux and (b) rejection% for MMMs membrane at constant oil concentration 158.28 ppm and pressure 3.5 bar

3.5 Effect of oil concentration, pressure, and HSP additives on oil response flux and rejection %

The oil response flux and rejection % may be represented like a solid with three dimensions. Figures 6, 7, and 8 show the permeate and rejection % flux with the two parameters. The primary goal of the response surface plot aims to determine the optimal operation factors, which can be expressed by the oil concentration, pressure, and additives concentration HSP NPs (wt.%), resulting in the maximum flux of permeate and rejection % for the oil/water emulsion. Figure 6a shows the response surface plot, illustrating the influence of oil concentration and pressure on the oil/water flux.

Figure 6a indicates that when the pressure is reduced and the oil concentration increases, the oil/water flux is reduced. A decrease in the pressure from 3.5 to 1.5 resulted in a substantial reduction in the flux, although a rise in the oil concentration was less effective than the pressure and resulted in a minor decrease in the flux. Figure 6b response surface plot shows how pressure and oil concentration affect the oil/water rejection %. Increasing the pressure caused a small reduction in membrane rejection, which had a negative impact on rejection. Thus, a rise in pressure can lead to some deformation in the polymer chains and increase pore size [61]. As a result, the rejection rate decreased at greater pressures, whereas increasing the oil concentration is increased by the rejection %. The increase in rejection can be attributed to the oil molecules on the membrane surface, which can create a thin, compact layer, raising the total rejection rate. Even so, the absence of interaction between these factors is attributed to the parallel straight lines structure of the contour plots.

Figure 7a displays a response surface plot illustrating the impact of oil concentration and additive content on the oil/water flux at a constant pressure.

The oil/water flux response demonstrated a reduction in the oil concentration and a rise in the additive concentration to 0.03wt.% resulted in higher flux. The greatest flux was recorded over 117 LMH with 0.03 wt.% of HSP NPs added. Increasing the concentration of HSP-NPs in the PLA/PBAT cast solution enhanced the membrane's porosity, average pore size, and hydrophilicity.

On the other hand, raising the content of additives to 0.05 wt.% reduced the flux due to the HSP-NPs agglomeration on the surface of PLA/PBAT membranes, resulting in lower porosity, pore size, and hydrophilicity [62]. The oil rejection% response indicated that increasing the additive content to 0.03wt.% and decreasing the oil concentration resulted in a lower rejection% at constant pressure, as illustrated in Figure 7b. The elliptical contour plots indicate an interaction between the oil content and additive concentration.

Figure 8a displays a three-dimensional plot of the response surface illustrating the impact of the coupling of the interaction between the additive concentration and the pressure on the oil/water flux at a constant oil concentration of 158.28 ppm and increasing the additive content to 0.03wt.% increased the oil/water flux more than the pressure. In general, an increase in flux

is caused by the combined effect of increasing the HSP-NPs content in the PLA/PBAT solution, increasing the hydrophilicity, average pore size, and porosity of the membrane, and raising the pressure, the permeate flux is increased due to higher shear stress on the surface of the membrane [63].

The response surface plot in Figure 8b depicts the influence between additive concentration and pressure on rejection % at constant oil concentration. Increasing the additive concentration to 0.03 wt.% enhanced rejection while increasing the pressure decreased rejection. However, raising the additive concentration to 0.03 wt.% enhanced rejection, even under high pressure. Additionally, the elliptical form of the contour plots leads to a noticeable interaction between the additive concentration and the pressure.

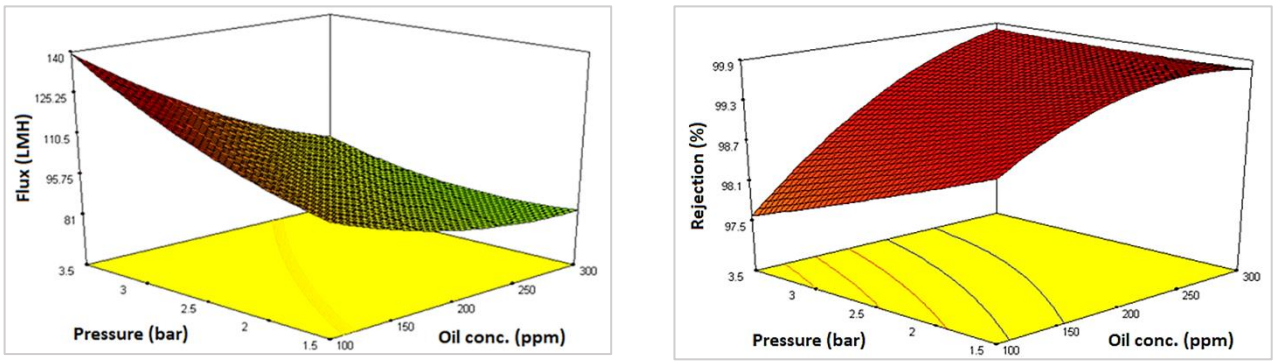

(a) **(b)**

Figure 6: Effect of pressure and concentration of oil for (**a**) flux and (**b**) rejection (%) at additive concentration 0.03 wt.%

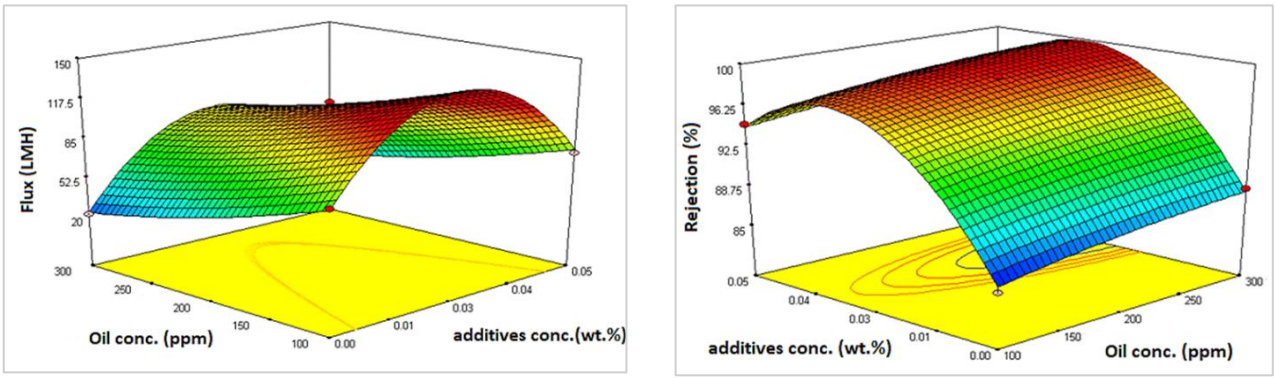

(a) **(b)**

Figure 7: concentration and concentration of oil for (**a**) flux and (**b**) rejection (%) at pressure 3.5 bar

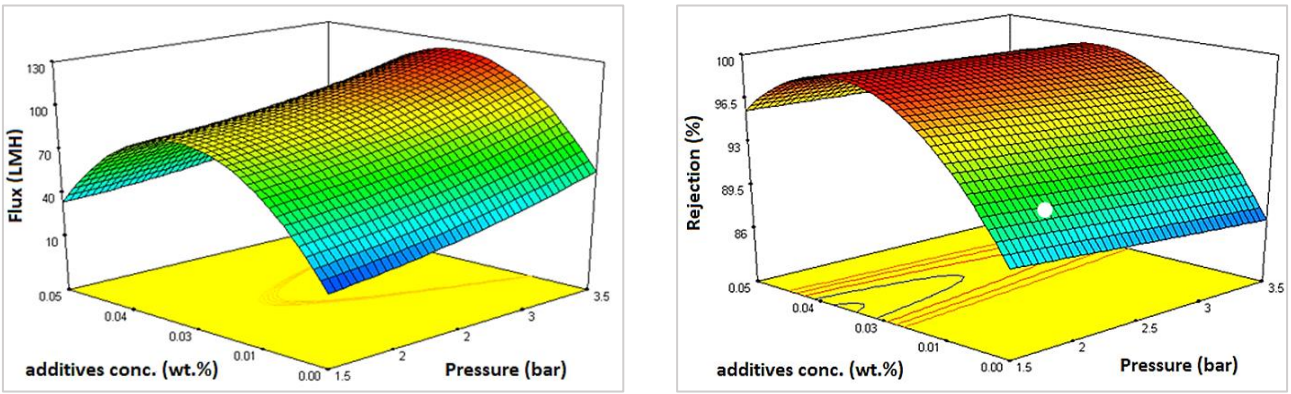

(a) **(b)**

Figure 8: Effect of additive concentration and pressure for (**a**) flux and (**b**) rejection (%) at oil concentration 158.28 ppm

3.6 Prediction of membrane performance

A linear regression function was used in Design-Expert® software to generate a prediction of the flux and rejection %. Figure 9 depicts the predicted and actual findings for the flux of permeate and rejection of oil %.

Thus, the membrane flux and rejection % of actual and predicted values are in strong mathematical agreement as shown in Figures 9a and 9b, respectively. The above finding and the high R2 (i.e., 99.76% and 99.64% of flux and rejection%) of the HSP membrane show the model's significant potential for predicting and optimizing flux and rejection percentages [66].

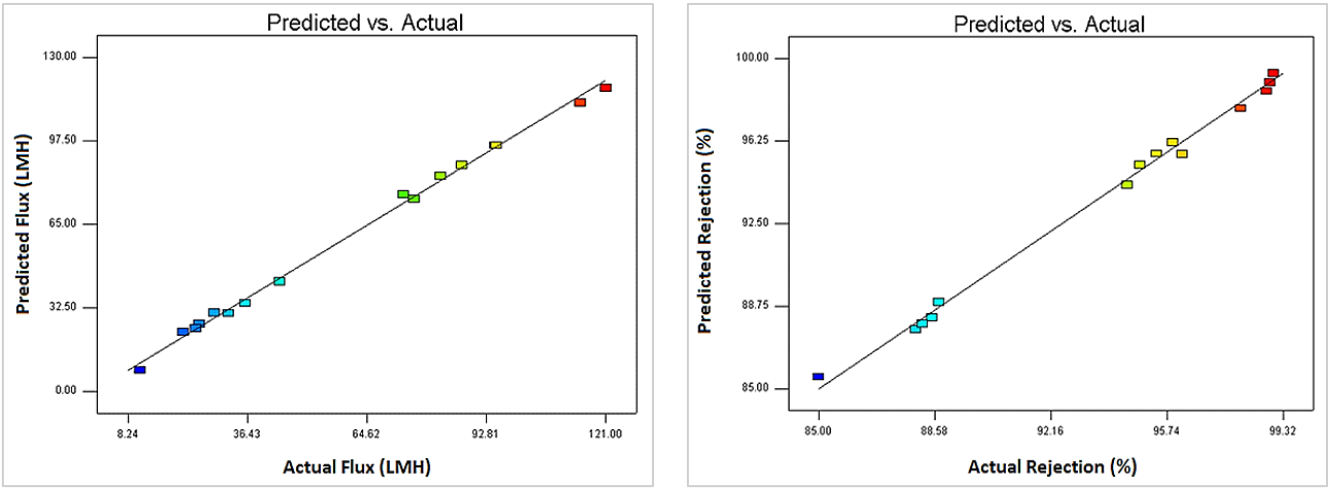

(a) **(b)**

Figure 9: Predicted and actual results for the (a) flux and (b) rejection %

3.7 Optimization and validity of the UF process

The desired function technique is one of the most prominent methods for optimizing various response processes within applied engineering and science domains. The method combines the responses to individual desirability from a single value within a scale ranging from one to zero. Because one value reflects the optimum scenario, values closer to one are chosen when defining the optimal conditions for operation. In contrast, when the result is near zero, all or some responses fall outside the intended range [67]. So, the desirability function for the two present responses (flux and rejection %) was determined utilizing Design-Expert® software, integrating the individual desirability to a single value, as seen in Figure 10. Since it had been estimated that the three of these variables were to significantly enhance the flux of oil/water and rejection factor, the following figure contains the optimal operating conditions tested (i.e., oil concentration, pressure, and additive concentration).

Furthermore, the flux and rejection % experiments were conducted at the suggested optimal operation conditions using the model to validate it. Table 6 indicates a 2.89% error between the predicted flux (121 LMH) and the experimental value (117.6 LMH) for membranes. Additionally, there was a 0.93% error between the predicted rejection % (98.53) and the experimental value (97.62). The small percentage error proves the significance and applicability of the created RSM model [68].

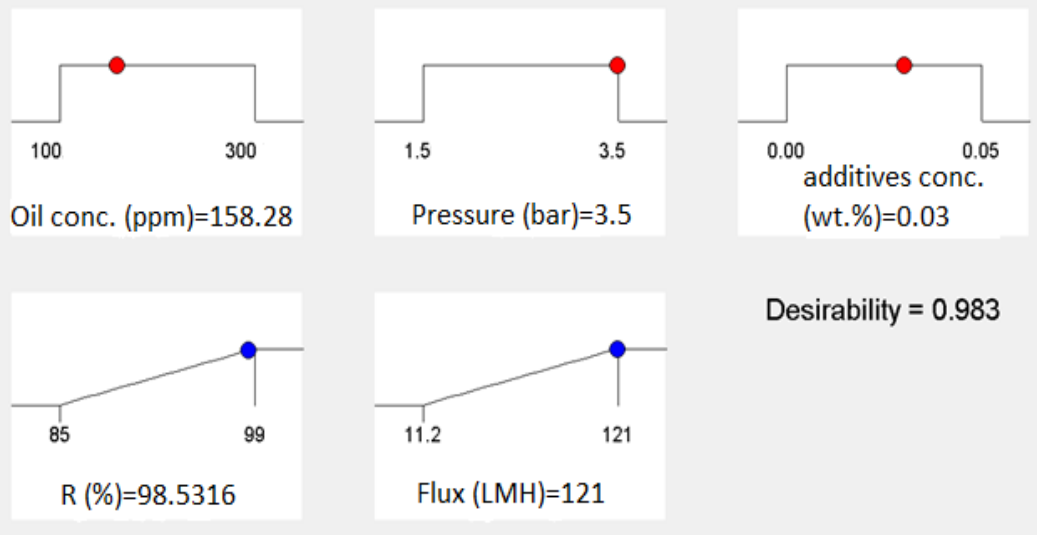

Figure 10: Desirability ramp for the numerical optimization of three chosen factors

Table 6: Predicted versus experimental values of the flux and rejection % under optimum conditions

Oil conc. (ppm)	Press. (bar)	Add. conc. (wt.%)	R. (%) Pred.	R. (%) Exp.	Error %	F(LMH)Pred.	F(LMH) Exp.	Error %
158.28	3.5	0.03	98.5316	97.62	0.93	121	117.6	2.89

4. Conclusion

The present research studied the influence of incorporated HSP NPs into PLA/PBAT MMMs for removing oil using simulating oily wastewater. Response surface methodology (RSM) and variance analysis (ANOVA) have been used as

statistical and mathematical methods to improve the technique's efficacy at a larger scale. An optimization study was conducted to determine the influence of operational variables on the flux and rejection of oil of PLA/PBAT/HSP membranes in the ultrafiltration method. The factors indicated that the highest effect on the flux and rejection of oil included the HSP NPs wt.%, oil concentration, and transmembrane pressure. The experimental design enabled the investigation of the effects of three oil concentrations. The flux and rejection % were analyzed using Design-Expert® software. A mathematical methodology for determining the flux and rejection % was developed. The findings indicate that factors have combined impacts on flux and rejection %. The optimized parameters display the membrane flux is 121 LMH and rejection % is 98.5316, at an HSP wt.% of 0.03%, an oil concentration of 158.28 ppm, and a pressure of 3.5 bar.

Acknowledgment

Acknowledgments may be directed to individuals or institutions that have contributed to the research or a government agency.

Author contributions

Conceptualization, M. Ghadhban and K. Rashid; data curation, M. Ghadhban, K. Rashid, and A. Abdulrazak.; formal analysis, H. Meskher and , Q. Alsalhy.; investigation, H. Meskher, Q. Alsalhy, and Y. Benguerba.; methodology, M. Ghadhban, K. Rashid, and E. Yousif Al-Sarraj.; software, M. Ghadhban and K. Rashid.; supervision, Q. Alsalhy.; validation, H. Meskher, and Q. Alsalhy.; visualization, Q. Alsalhy, and Y. Benguerba.; writing—original draft preparation, M. Ghadhban, and K. Rashid.; writing—review and editing, M. Ghadhban, K. Rashid, and H. Meskher. All authors have read and agreed to the published version of the manuscript.

Funding

This research received no specific grant from any funding agency in the public, commercial, or not-for-profit sectors.

Data availability statement

The data that support the findings of this study are available on request from the corresponding author.

Conflicts of interest

Authors have no conflicts of interest to declare.

References

[1] K. T. Rashid, H. M. Alayan, A. E. Mahdi, M. N. Al-Baiati, H. Sh. Majdi, I. K. Salih, J. M. Ali, Q. F. Alsalhy, Novel Water-Soluble Poly(terephthalic-co-glycerol-g-fumaric acid) Copolymer Nanoparticles Harnessed as Pore Formers for Polyethersulfone Membrane Modification: Permeability–Selectivity Tradeoff Manipulation, Water, 14 (2022) 1507. https://doi.org/10.3390/w14091507

[2] Q. F. Alsalhy, A. A. Mohammed, S. H. Ahmed, K. T. Rashid, and M. A. AlSaadi, Estimation of nanofiltration membrane transport parameters for cobalt ions removal from aqueous solutions, Desalin. Water Treat., 108 (2018) 235-245. https://doi.org/10.5004/dwt.2018.21929

[3] G. M. Jaid, A. A. AbdulRazak, H. Meskher, S. Al-Saadi, Q. F. Alsalhy, Metal-organic frameworks (MOFs), covalent organic frameworks (COFs), and hydrogen-bonded organic frameworks (HOFs) in mixed matrix membranes, Mater. Today Sustain., 25 (2024) 100672. https://doi.org/10.1016/j.mtsust.2024.100672

[4] H. Meskher, S.B. Belhaouari, K. Deshmukh, C.M. Hussain, F. Sharifianjazi, A Magnetite Composite of Molecularly Imprinted Polymer and Reduced Graphene Oxide for Sensitive and Selective Electrochemical Detection of Catechol in Water and Milk Samples: An Artificial Neural Network (ANN) Application, J. Electrochem. Soc,. 170 (2023) 047502. https://doi.org/10.1149/1945-7111/acc97c.

[5] H. Meskher, A. K. Thakur, F. Sharifianjazi, R. Sathyamurthy, I. Lynch, R. Saidur, MXene-CNTs: A Prospective Composite Material for Biomedical Applications Engrossing Wearable Sensors , in ACS Symposium Series, 1443, 2023, 61-83. https://doi.org/10.1021/bk-2023-1443.ch004

[6] M. Y. Ghadhban, K. T. Rashid, A. A AbdulRazak, and Q. F. Alsalhy, Recent progress and future directions of membranes green polymers for oily wastewater treatment, Water Sci. Technol., 87 (2023) 57-82. https://doi.org/10.2166/wst.2022.409

[7] A. I. Adetunji and A. O. Olaniran, Treatment of industrial oily wastewater by advanced technologies: a review, Appl. Water Sci., 11 (2021) 1-19. https://doi.org/10.1007/s13201-021-01430-4

[8] A. H. Behroozi and M. R. Ataabadi, Improvement in microfiltration process of oily wastewater: A comprehensive review over two decades, J. Environ. Chem. Eng., 9 (2021) 104981. https://doi.org/10.1016/j.jece.2020.104981

[9] S.T. Abdul-Hussein, M.H. Al-Furaiji, H. Meskher, D. Ghernaout, M. Fal, A.M. ALotaibi, Q.F. Alsalhy, Prospects of forward osmosis-based membranes for seawater mining: Economic analysis, limitations and opportunities, *Desalination*, vol. 579, 2024, 117477. https://doi.org/10.1016/j.desal.2024.117477

[10] M. A. Qamar, M. Javed, S. Shahid, and M. Sher, Fabrication of g-C3N4/transition metal (Fe, Co, Ni, Mn and Cr)-doped ZnO ternary composites: Excellent visible light active photocatalysts for the degradation of organic pollutants from wastewater, Mater. Res. Bull., 147 (2022) 111630. https://doi.org/10.1016/j.materresbull.2021.111630

[11] É. Nascimbén Santos, Z. László, C. Hodúr, G. Arthanareeswaran, and G. Veréb, Photocatalytic membrane filtration and its advantages over conventional approaches in the treatment of oily wastewater: A review, Asia-Pacific J. Chem. Eng., 15 (2020) 1-29. https://doi.org/10.1002/apj.2533

[12] J. M. Shihab, K. T. Rashid, and M. A. Toma, A review on membrane technology application for vegetable oil purification processes, Int. J. Food Eng., 18 (2022) 655-677. https://doi.org/10.1515/ijfe-2022-0058

[13] F. Kazemi, Y. Jafarzadeh, S. Masoumi, and M. Rostamizadeh, Oil-in-water emulsion separation by PVC membranes embedded with GO-ZnO nanoparticles, J. Environ. Chem. Eng., 9 (2021) 104992. https://doi.org/10.1016/j.jece.2020.104992

[14] H. Meskher, F. Achi, Electrochemical Sensing Systems for the Analysis of Catechol and Hydroquinone in the Aquatic Environments: A Critical Review, Crit. Rev. Anal. Chem. (2022) 1–14. https://doi.org/10.1080/10408347.2022.2114784.

[15] M. Y. Ghadhban, K. T. Rashid, A. A. Abdulrazak, I. T. Ibrahim, Q. F. Alsalhy, Z. M. Shakor, I. Hamawand, Banana Peel Additives for Oil Wastewater Treatment, 16 (2024) 1040. https://doi.org/10.3390/w16071040

[16] F. Yalcinkaya, E. Boyraz, J. Maryska, and K. Kucerova, A review on membrane technology and chemical surface modification for the oily wastewater treatment, Materials (Basel)., 13 (2020) 493. https://doi.org/10.3390/ma13020493

[17] C. J. Singh, S. Mukhopadhyay, and R. S. Rengasamy, Fibrous coalescence filtration in treating oily wastewater: A review, J. Ind. Text., 51 (2022). https://doi.org/10.1177/15280837211040863

[18] E. S. Dmitrieva, T. S. Anokhina, E. G. Novitsky, V. V. Volkov, A. V. Volkov, and I. L. Borisov, Polymeric Membranes for Oil-Water Separation: A Review, Polymers (Basel)., 14 (2022) 1-25. https://doi.org/10.3390/polym14050980

[19] A. Mohamed and S. Yousef, "Green and sustainable membrane fabrication development, Sustain. Technol. Green Econ., 1, (2021)14-23. https://doi.org/10.21595/stge.2021.22126

[20] S. Gadlula, L. N. Ndlovu, N. R. Ndebele, and L. K. Ncube, Membrane technology in tannery wastewater management: A review, Zimbabwe J. Sci. Technol., 14 (2019) 57-72.

[21] S. A. Rahman, K. T. Rashid, and Q. F. Alsalhy, Improvement of PVDF-co-HFP Hollow Fiber Membranes for Direct Contact Membrane Distillation Applications, Indian J. Sci. Technol., 10 (2017) 1-5. https://doi.org/10.17485/ijst/2017/v10i7/111446

[22] V. Vasagar, M. K. Hassan, and M. Khraisheh, Membrane surface modification and functionalization, Membranes, 11 (2021) 877. https://doi.org/10.3390/membranes11110877

[23] H. Meskher, S.B. Belhaouari, F. Sharifianjazi, Mini review about metal-organic framework (MOF)-based wearable sensors: Challenges and prospects, Heliyon, 9 (2923) e21621. https://doi.org/10.1016/j.heliyon.2023.e21621

[24] K. M. Shabeeb, K. M. Shabeeb,W. A. Noori, A. A. Abdulridha, H. Sh. Majdi, M. N. Al-Baiati, A. A. Yahya, K. T. Rashid, Z. Németh, K. Hernadi, Q. F. Alsalhy, Novel partially cross-linked nanoparticles graft co-polymer as pore former for polyethersulfone membranes for dyes removal, Heliyon, 9 (2023) 1-17. https://doi.org/10.1016/j.heliyon.2023.e21958

[25] H. Meskher, H.C. Mustansar, A.K. Thakur, R. Sathyamurthy, I. Lynch, P. Singh, T. K. Han, R. Saidur, Recent trends in carbon nanotube (CNT)-based biosensors for the fast and sensitive detection of human viruses: a critical review, Nanoscale Adv., 5 (2023) 992-1010. https://doi.org/10.1039/D2NA00236A

[26] M. A. Qamar, M. Javed, S. Shahid, M. Shariq, M. M. Fadhali, S. K. Ali, M. Sh. Khan, Synthesis and applications of graphitic carbon nitride (g-C3N4) based membranes for wastewater treatment: A critical review, Heliyon, 9 (2023) e12685. https://doi.org/10.1016/j.heliyon.2022.e12685

[27] M. A. Qamar, S. Shahid, and M. Javed, Synthesis of dynamic g-C3N4/Fe@ZnO nanocomposites for environmental remediation applications, Ceram. Int., 46 (2020) 22171-22180. https://doi.org/10.1016/j.ceramint.2020.05.294

[28] T. W. Abood, K. M. Shabeeb, A. B. Alzubaydi, H. Meskher , A. K. Lafta , R. A. Al-Juboori , F. Sharifianjazi, K. Hernadi, Q. F. Alsalhy, MXene-based pressure driven membranes for wastewater treatment: A critical review, Desalination Water Treat., 320, (2024) 100594. https://doi.org/10.1016/j.dwt.2024.100594

[29] V. Marturano, A. Marotta, S. A. Salazar, V. Ambrogi, and P. Cerruti, Recent advances in bio-based functional additives for polymers, Prog. Mater. Sci., 139 (2022) 101186. https://doi.org/10.1016/j.pmatsci.2023.101186

[30] Y. Manawi, V. Kochkodan, E. Mahmoudi, D. J. Johnson, A. W. Mohammad, and M. A. Atieh, Characterization and Separation Performance of a Novel Polyethersulfone Membrane Blended with Acacia Gum, Sci. Rep., 7 (2017) 1-12. https://doi.org/10.1038/s41598-017-14735-9

[31] A. Fahrina, N. Arahman, S. Mulyati, S. Aprilia, and M. R. Bilad, Characterization of polyethersulfone (PES) membrane entrapping with ginger extract (GE) as a green additive, IOP Conf. Ser. Mater. Sci. Eng., 1087 (2021) 12050. https://doi.org/10.1088/1757-899x/1087/1/012050

[32] H. A. Le Phuong, N. A. Izzati Ayob, C. F. Blanford, N. F. Mohammad Rawi, and G. Szekely, Nonwoven Membrane Supports from Renewable Resources: Bamboo Fiber Reinforced Poly(Lactic Acid) Composites, ACS Sustain. Chem. Eng., 7 (2019) 11885-11893. https://doi.org/10.1021/acssuschemeng.9b02516

[33] H. Idress, S. Z. J. Zaidi, A. Sabir, M. Shafiq, R. U. Khan, C. Harito, S. Hassan & F. C. Walsh, Cellulose acetate based Complexation-NF membranes for the removal of Pb(II) from waste water, Sci. Rep., 11 (2021) 1-14. https://doi.org/10.1038/s41598-020-80384-0

[34] N. Rabiee, Rajni Sharma, Sahar Foorginezhad, Maryam Jouyandeh, Mohsen Asadnia, Mohammad Rabiee, Omid Akhavan, Eder C. Lima, Krzysztof Formela, Milad Ashrafizadeh, Zari Fallah, Mahnaz Hassanpour, Abbas Mohammadi, Mohammad Reza Saeb, Green and Sustainable Membranes: A review, Environ. Res., 231 (2023) 116133. https://doi.org/10.1016/j.envres.2023.116133

[35] R. I. Raja, K. T. Rashid, M. A. Toma, A. A. AbdulRazak, M. Ahmed Shehab, and K. Hernadi, A Novel Polyethersulfone/Chamomile (PES/Chm) Mixed Matrix Membranes for Wastewater Treatment Applications, J. Saudi Chem. Soc., 28 (2024) 101805. https://doi.org/10.1016/j.jscs.2023.101805

[36] J. M. Shihab, M. A. Toma, A. D. Hussein, and K. T. Rashid, Green Agents as Alternative to N-Hexane for Sunflower Vegetable Oil Degumming and Deacidification via Ultrafiltration Membrane, Chem. Africa, 7 (2024) 281-290. https://doi.org/10.1007/s42250-023-00757-6

[37] M. Malhotra, M. Pal, and P. Pal, A response surface optimized nanofiltration-based system for efficient removal of selenium from drinking Water, J. Water Process Eng., 33 (2019) 101007. https://doi.org/10.1016/j.jwpe.2019.101007

[38] J. Rajewski and A. Dobrzyńska-Inger, Application of response surface methodology (Rsm) for the optimization of chromium(iii) synergistic extraction by supported liquid membrane, Membranes (Basel)., 11 (2021) https://doi.org/10.3390/membranes11110854

[39] M. Inger, A. Dobrzyńska-Inger, J. Rajewski, and M. Wilk, The use of response surface methodology in ammonia oxidation reaction study, J. Chem., 2019 (2019). https://doi.org/10.1155/2019/2641315

[40] Z. M. Shakor, A. A. AbdulRazak, and A. A. Shuhaib, Optimization of process variables for hydrogenation of cinnamaldehyde to cinnamyl alcohol over a Pt/SiO2 catalyst using response surface methodology, Chem. Eng. Commun. 209 (2022) 827-843. https://doi.org/10.1080/00986445.2021.1922394

[41] F. Al-Sheikh, F. T. Jasim, Sh. T. Al-Humairi, I. Hussein, A. A. AbdulRazak, Z. M. Shakor & S. Rohani, Adsorption of Blue Cationic Thiazine Dye from Synthetic Wastewater by Natural Iraqi Bentonite Using Response Surface Methodology: Isotherm, Kinetic, and Thermodynamic Studies, Chem. Africa, 6 (2023) 1437-1447. https://doi.org/10.1007/s42250-023-00591-w

[42] M. Y. Ghadhban, K. T. Rashid, A. A. Abdulrazak, and Q. F. Alsalhy, A novel poly (lactic-acid) and poly (butylene adipate-co-terephthalate) blend membrane modified with hesperidin for oily water emulsions separation, Chem. Eng. Res. Des., 206 (2024) 265-279. https://doi.org/10.1016/j.cherd.2024.05.020

[43] K. Keawsupsak, Arisa Jaiyu, Julaluk Pannoi, Punthinee Somwongsa, Nopparat Wanthausk, Passakorn Sueprasita, Chutima Eamchotchawalit, Poly(lactic acid)/Biodegradable Polymer Blend for The Preparation of Flat-Sheet Membrane, J. Teknologi, 69 (2014). https://doi.org/10.11113/jt.v69.3405

[44] K. Valizadeh, A. Heydarinasab, S. S. Hosseini, and S. Bazgir, Preparation of modified membrane of polyvinylidene fluoride (PVDF) and evaluation of anti-fouling features and high capability in water/oil emulsion separation, J. Taiwan Inst. Chem. Eng., 126 (2021) 36-49. https://doi.org/10.1016/j.jtice.2021.07.018

[45] Q. F. Alsalhy, A. Merza, K. T. Rashid, A. Adam, A. Figoli, S. Simone, E. Drioli, Preparation and characterization of poly(vinyl chloride)/polystyrene/ poly(ethylene glycol) hollow-fiber ultrafiltration membranes, J. Appl. Polym. Sci., 130 (2013) 989-1004. https://doi.org/10.1002/app.39221

[46] X. Zhang, C. Wei, Sh. Ma, C. Zhang, Y. Li, D. Chen, Z. Xu, X. Huang., Janus poly (vinylidene fluoride)-graft-(TiO_2 nanoparticles and PFDS) membranes with loose architecture and asymmetric wettability for efficient switchable separation of surfactant-stabilized oil/water emulsions, J. Memb. Sci., 640 (2021) 119837. https://doi.org/10.1016/j.memsci.2021.119837

[47] X. Zhu, Z. Yu, H. Zeng, X. Feng, Y. Liu, K. Cao, X. Li, R. Long, Using a simple method to prepare UiO-66-NH2/chitosan composite membranes for oil–water separation, J. Appl. Polym. Sci., 138 (2021) https://doi.org/10.1002/app.50765

[48] I. Veza, M. Spraggon, I. M. R. Fattah, and M. Idris, Response surface methodology (RSM) for optimizing engine performance and emissions fueled with biofuel: Review of RSM for sustainability energy transition, Results Eng., 18 (2023) 101213. https://doi.org/10.1016/j.rineng.2023.101213

[49] A. A. Abdulrazak, Z. M. Shakor, and S. Rohani, Optimizing Biebrich Scarlet removal from water by magnetic zeolite 13X using response surface method, J. Environ. Chem. Eng., 6 (2018) 6175-6183. https://doi.org/10.1016/j.jece.2018.09.043

[50] Y. Guo, Q. Xue, H. Zhang, N. Wang, S. Chang, H. Wang, H. Pangb and H. Chen, Treatment of real benzene dye intermediates wastewater by the Fenton method: Characteristics and multi-response optimization, RSC Adv., 8 (2018) 80-90. https://doi.org/10.1039/c7ra09404c

[51] B. Jabbari, E. Jalilnejad, K. Ghasemzadeh, and A. Iulianelli, Modeling and optimization of a membrane gas separation based bioreactor plant for biohydrogen production by CFD–RSM combined method, J. Water Process Eng., 43 (2021) 102288. https://doi.org/10.1016/j.jwpe.2021.102288

[52] S. Waqas, N. Y. Harun, U. Arshad, A. M. Laziz, S. L. S. Mun, M. R. Bilad, N. A. H. Nordin, A. S. Alsaadi, Optimization of operational parameters using RSM, ANN, and SVM in membrane integrated with rotating biological contactor, Chemosphere, 349 (2024) 140830. https://doi.org/10.1016/j.chemosphere.2023.140830

[53] V. Vatanpour, S. S. Madaeni, A. R. Khataee, E. Salehi, S. Zinadini, and H. A. Monfared, TiO_2 embedded mixed matrix PES nanocomposite membranes: Influence of different sizes and types of nanoparticles on antifouling and performance, Desalination, 292 (2012) 19-29. https://doi.org/10.1016/j.desal.2012.02.006

[54] K. T. Rashid, S. B. A. Rahman, and Q. F. Alsalhy, Optimum Operating Parameters for Hollow Fiber Membranes in Direct Contact Membrane Distillation, Arab. J. Sci. Eng., 41 (2016) 2647-2658. https://doi.org/10.1007/s13369-016-2178-3

[55] Z. Majid, A. A. AbdulRazak, and W. A. H. Noori, Modification of Zeolite by Magnetic Nanoparticles for Organic Dye Removal, Arab. J. Sci. Eng., 44 (2019) 5457-5474. https://doi.org/10.1007/s13369-019-03788-9

[56] K. C. Ho, Y. H. Teow, W. L. Ang, and A. W. Mohammad, Novel GO/OMWCNTs mixed-matrix membrane with enhanced antifouling property for palm oil mill effluent treatment, Sep. Purif. Technol., 177 (2017) 337-349. https://doi.org/10.1016/j.seppur.2017.01.014

[57] D. Da Silva Biron, M. Zeni, C. P. Bergmann, and V. Dos Santos, Analysis of composite membranes in the separation of emulsions sunflower oil/water, Mater. Res., 20 (2017) 843-852. https://doi.org/10.1590/1980-5373-MR-2016-0732

[58] Y. J. Lim, S. M. Lee, R. Wang, and J. Lee, Emerging materials to prepare mixed matrix membranes for pollutant removal in water, Membranes , 11 (2021) 508. https://doi.org/10.3390/membranes11070508

[59] M. R. S. Kebria, M. Jahanshahi, and A. Rahimpour, SiO<inf>2</inf> modified polyethyleneimine-based nanofiltration membranes for dye removal from aqueous and organic solutions, Desalination, 367 (2015) 255-264. https://doi.org/10.1016/j.desal.2015.04.017

[60] T. Mohammadi and A. Esmaeelifar, Wastewater treatment of a vegetable oil factory by a hybrid ultrafiltration-activated carbon process, J. Memb. Sci., 254 (2005) 129-137. https://doi.org/10.1016/j.memsci.2004.12.037

[61] A. Hussain and M. Al-Yaari, Development of polymeric membranes for oil/water separation, Membranes (Basel)., 11 (2021) 1-15. https://doi.org/10.3390/membranes11010042

[62] T. K. Abbas, K. T. Rashid, and Q. F. Alsalhy, NaY zeolite-polyethersulfone-modified membranes for the removal of cesium-137 from liquid radioactive waste, Chem. Eng. Res. Des., 179 (2022) 535-548. https://doi.org/10.1016/j.cherd.2022.02.001

[63] S. M. Hosseini, M. Afshari, A.R. Fazlali, S. K. Farahani, S. Bandehali, B. V. Bruggen, E. Bagheripour, Mixed matrix PES-based nanofiltration membrane decorated by (Fe3O4–polyvinylpyrrolidone) composite nanoparticles with intensified antifouling and separation characteristics, Chem. Eng. Res. Des., 147 (2019) 390-398. https://doi.org/10.1016/j.cherd.2019.05.025

[64] A. Najjar, S. Sabri, R. Al-Gaashani, V. Kochkodan, and M. A. Atieh, Enhanced fouling resistance and antibacterial properties of novel graphene oxide-arabic gum polyethersulfone membranes, Appl. Sci., 9 (2019). https://doi.org/10.3390/app9030513

[65] C. N. Matindi, S. Kadanyo, G. Liu, M. Hu, Y. Hu, Z. Cui, , X. Ma, F. Yan, B. He, J. Li, Hydrophilic polyethyleneimine-TiO_2 hybrid layer on polyethersulfone/sulfonated polysulfone blend membrane with antifouling characteristics for the

effective separation of oil-in-water emulsions, J. Water Process Eng., 49 (2022) 102982. https://doi.org/10.1016/j.jwpe.2022.102982

[66] S. H. Rasheed, S. S. Ibrahim, Q. F. Alsalhy, and I. K. Salih, Separation of Soluble Benzene from an Aqueous Solution by Pervaporation Using a Commercial Polydimethylsiloxane Membrane, Membranes (Basel)., 12 (2022). https://doi.org/10.3390/membranes12111040

[67] S. H. Rasheed, S. S. Ibrahim, Q. F. Alsalhy, and H. S. Majdi, Polydimethylsiloxane (PDMS) Membrane for Separation of Soluble Toluene by Pervaporation Process, Membranes (Basel)., 13 (2023). https://doi.org/10.3390/membranes13030289

[68] D. A. Hussein Al-Timimi, Q. F. Alsalhy, A. A. AbdulRazak, M. A. Shehab, Z. Németh, and K. Hernadi, Optimum operating parameters for PES nanocomposite membranes for mebeverine hydrochloride removal, J. Mater. Res. Technol., 24 (2023) 6779-6790. https://doi.org/10.1016/j.jmrt.2023.04.247